Influence of evanescent wave on birefringent microplates

Angelsky, O. V.; Hanson, Steen Grüner; Maksimyak, P. P.; Maksimyak, A. P.; Zenkova, C. Yu.; Polyanskii, P. V.; Ivanskyi, D. I.

Published in:
Optics Express

Link to article, DOI:
10.1364/OE.25.002299

Publication date:
2017

Document Version
Publisher's PDF, also known as Version of record

Research Article | Vol. 25, No. 3 | 6 Feb 2017 | OPTICS EXPRESS 2299

Optics EXPRESS

Influence of evanescent wave on birefringent microplates

O. V. ANGELSKY,[1] S. G. HANSON,[2] P. P. MAKSIMYAK,[1] A. P. MAKSIMYAK,[1] C. YU. ZENKOVA,[1] P. V. POLYANSKII,[1] AND D. I. IVANSKYI[1]

[1]*Correlation Optics Department, Chernivtsi National University, 2, Kotsyubinsky Str., Chernivtsi 58012,Ukraine*
[2]*DTU Fotonik, Department of Photonics Engineering, DK-4000 Roskilde, Denmark*
[*]*o.angelsky@chnu.edu.ua*

Abstract: Mechanical action caused by the optical forces connected with the canonical momentum density associated with the local wavevector or Belinfante's spin angular momentum is experimentally verified. The helicity-dependent and the helicity-independent forces determined by spin momenta of different nature open attractive prospects for the use of optical structures for manipulating minute quantities of matter of importance in nanophysics, nanooptics and nanotechnologies, precision chemistry and pharmacology and in numerous other areas. Investigations in this area reveal new, extraordinary manifestations of optical forces, including the helicity-independent force caused by the transverse helicity-independent spin or vertical spin of a diagonally polarized wave, which was not observed and exploited up to recently. The main finding of our study consists in a direct experimental demonstration of the physical existence and mechanical action of this recently discovered extraordinary transverse component of the spin here arising in an evanescent light wave due to the total internal reflection of a linearly polarized probing beam with azimuthal angle 45° at the interface between the birefringent plate and air, which is oriented perpendicularly to the wavevector of an evanescent wave and localized over the boundary of the transparent media with polarization-dependent refraction indices.

OCIS codes: (260.2160) Energy transfer; (260.5430) Polarization; (350.4855) Optical tweezers or optical manipulation; (350.4990) Particles.

References and links

1. H. C. Ohanian, "What is spin?" Am. J. Phys. **54**(6), 500–505 (1986).
2. M.V. Berry, "Optical currents," J. Opt. A: Pure Appl. Opt. **11**, 094001 (2009).
3. L. Allen, M. W. Beijersbergen, R. J. Spreeuw, and J. P. Woerdman, "Orbital angular momentum of light and the transformation of Laguerre-Gaussian laser modes," Phys. Rev. A **45**(11), 8185–8189 (1992).
4. L. Allen and M. J. Padgett, "The Poynting vector in Laguerre–Gaussian beams and the interpretation of their angular momentum density," Opt. Commun. **184**(1–4), 67–71 (2000).
5. O. V. Angelsky, A. Ya. Bekshaev, P. P. Maksimyak, A. P. Maksimyak, I. I. Mokhun, S. G. Hanson, C. Yu. Zenkova, and A. V. Tyurin, "Circular motion of particles suspended in a Gaussian beam with circular polarization validates the spin part of the internal energy flow," Opt. Express **20**(10), 11351–11356 (2012).
6. O. V. Angelsky, A. Ya. Bekshaev, P. P. Maksimyak, A. P. Maksimyak, S. G. Hanson, and C. Yu. Zenkova, "Orbital rotation without orbital angular momentum: mechanical action of the spin part of the internal energy flow in light beams," Opt. Express **20**(4), 3563–3571 (2012).
7. A. Ashkin, "History of optical trapping and manipulation of small-neutral particle, atoms, and molecules," IEEE J. Sel. Top. Quantum Electron. **6**(6), 841–856 (2000).
8. D. G. Grier, "A revolution in optical manipulation," Nature **424**(6950), 810–816 (2003).
9. A. Ashkin and J. P. Gordon, "Stability of radiation-pressure particle traps: an optical Earnshaw theorem," Opt. Lett. **8**(10), 511–513 (1983).
10. S. M. Barnett and M. V. Berry, "Super weak momentum transfer near optical vortices," J. Opt. **15**(12), 125701 (2013).
11. M. Antognozzi, C. R. Bermingham, R. L. Harniman, S. Simpson, J. Senior, R. Hayward, H. Hoerber, M. R. Dennis, A. Y. Bekshaev, K. Y. Bliokh, and F. Nori, "Direct measurements of the extraordinary optical momentum and transverse spin-dependent force using a nano-cantilever," Nat. Phys. **12**(8), 731–735 (2016).
12. A. Aiello, P. Banzer, M. Neugebauer, and G. Leuchs, "From transverse angular momentum to photonic wheels," Nat. Photonics **9**(12), 789–795 (2015).

#280861 https://doi.org/10.1364/OE.25.002299
Journal © 2017 Received 1 Dec 2016; revised 16 Jan 2017; accepted 16 Jan 2017; published 27 Jan 2017

Optics EXPRESS

13. K. Y. Bliokh, F. J. Rodríguez-Fortuño, F. Nori, and A. V. Zayats, "Spin-orbit interactions of light,'," Nat. Photonics **9**(12), 796–808 (2015).
14. K. Y. Bliokh, A. Y. Bekshaev, and F. Nori, "Dual electromagnetism: helicity, spin, momentum, and angular momentum," New J. Phys. **15**(3), 033026 (2013).
15. M. Neugebauer, T. Bauer, A. Aiello, and P. Banzer, "Measuring the transverse spin density of light," Phys. Rev. Lett. **114**(6), 063901 (2015).
16. K. Y. Bliokh, A. Y. Bekshaev, and F. Nori, "Extraordinary momentum and spin in evanescent waves," Nat. Commun. **5**, 3300 (2014).
17. A. Aiello, N. Lindlein, C. Marquardt, and G. Leuchs, "Transverse angular momentum and geometric spin Hall effect of light," Phys. Rev. Lett. **103**(10), 100401 (2009).
18. K. Y. Bliokh and F. Nori, "Transverse spin of a surface plasmon," Phys. Rev. A **85**(6), 061801 (2012).
19. P. Banzer, M. Neugebauer, A. Aiello, C. Marquardt, N. Lindlein, T. Bauer, and G. Leuchs, "The photonic well-demonstration of a state of light with purely transverse angular momentum," J. Eur. Opt. Soc. Rap. Publ. **8**, 13032 (2013).
20. R. A. Beth, "Mechanical Detection and Measurement of the Angular Momentum of Light," Phys. Rev. **50**(2), 115–125 (1936).
21. C. Rockstuhl and H. P. Herzig, "Calculation of the torque on dielectric elliptical cylinders," J. Opt. Soc. Am. A **22**(1), 109–116 (2005).
22. M. E. J. Friese, T. A. Nieminen, N. R. Heckenberg, and H. Rubinsztein-Dunlop, "Optical alignment and spinning of laser-trapped microscopic particles," Nature **394**(6691), 348–350 (1998).
23. A. Ya. Bekshaev, O. V. Angelsky, S. V. Sviridova, and C. Yu. Zenkova, "Mechanical Action of Inhomogeneously Polarized Optical Fields and Detection of the Internal Energy Flows," Advances in Optical Technologies, Article ID 723901, 11 pages (2011).
24. A. Hayata, J. P. Balthasar Muellera, and F. Capassoa, "Lateral chirality-sorting optical forces," PNAS Early Edition, 5 pages (2015).

1. Introduction

A circularly polarized beam is an example of an optical beam possessing spin angular momentum (AM) [1]. The analysis and estimation of the magnitude of such AM are possible when the AM is transferred to a small particle by observing its rotational or rectilinear motion [2–10]. This feasibility is implemented for conventional, non-structured optical fields, i.e. plane, spherical waves etc. Other feasibilities are realized in the case of evanescent waves. As it has been shown in recent papers [11, 12], evanescent electromagnetic waves offer a rich and highly non-trivial structure of the local momentum and spin distributions. The transverse spin momentum turns out to be the fundamental spin momentum introduced by Belinfante in field theory [13]. By the way, the visualization of the action of the longitudinal (helicity-independent) Belinfante momentum was proposed in [14], which is associated with non-zero transverse spin density in optical vector beams. Uncommonness of the properties of evanescent waves generated by a linearly polarized probing wave manifests itself, in part, in the occurrence of the vertical spin, as it has recently been shown [15, 16], see also earlier relevant papers [17–19]. In a recent paper [11], direct measurement of an extraordinary optical momentum and helicity-dependent force directed perpendicularly to the wavevector being proportional to the ellipticity of the local polarization of the probing beam has been reported. Such an optical force takes place for evanescent waves and other structured fields being associated with the spin-momentum part of the Poynting vector. The extraordinary transverse momentum has been measured using a femto-newton resolution nano-cantilever immersed in an evanescent optical field above the total internal reflecting glass surface. Besides, it has been established that the transverse force exhibits another polarization-dependent contribution determined by the imaginary part of the complex Poynting vector.

It is obvious that the most convincing means for proving the existence and influence of any physical parameter is to directly demonstrate and visualize the resulting action caused by this parameter under natural conditions. This experimental approach is realized in this paper, being basically a variation of the classical "suspended plate" experiment by Beth [20]. Here, for the first time, we use a free-standing plate for detection of the influence of an evanescent wave.

Specifically, we demonstrate the motion of an optically transparent birefringent microplate influenced by the optical forces arising at the plate plane due to the optical forces caused by

Optics EXPRESS

simultaneous action of the canonical momentum directed along the wavevector and the transversal spin momentum [15] directed perpendicularly to the canonical momentum, causing the motion in the direction of the Poynting vector which does not coincide with any of these directions. The surfaces of a birefringent plate have negligible roughness. In order to transfer the transverse momentum to the plate we deposed gold nanoparticles at its upper surface.

To elucidate the main idea of our study, Fig. 1 shows a general view of the experimental arrangement. The detailed experimental arrangement will be represented in Section 2. The probing laser beam is oriented in such a manner that, after passing the glass prism 1 and cuvette 2 with liquid (water) 3, it impinges onto the small plate 4 made from transparent birefringent material at an angle exceeding the critical angle of the total internal reflection (TIR). As a result, an evanescent wave is excited just above the plate at the plate-air interface. Depending on the action imposed by the evanescent wave, the test plate can move rectilinearly or rotate. This motion can be visualized with CCD-camera 6 using the white-light illuminating source 5. In such a manner, we are in a position to perform direct and convincing visualization of the action of an evanescent wave with various parameters of the probing beam.

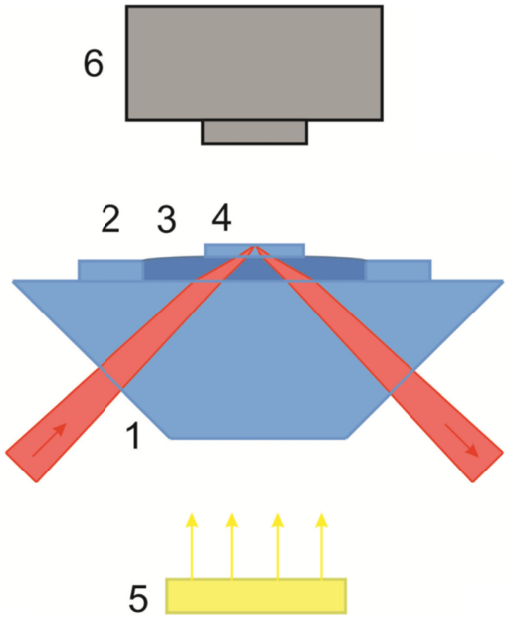

Fig. 1. Experimental arrangement: 1 – glass cut rectangular prism (n = 1.52); 2 – 2 mm-height ring cuvette; 3 – water (n = 1.33); 4 – plate with gold nanoparicles at its upper surface; 5 – white-light illuminating source; 6 – CCD-camera.

We show that specially arranged experimental conditions may be implemented ensuring that the contributions from the canonical and spin momenta in determining the trajectory of the resulting motion may become commensurable, while the chaotic motion of molecules in the water environment becomes negligible due to space averaging over the plate area. The influence of the surface tension of water is minimized due to the convex form of the meniscus. Commensurability of the contributions of the two mentioned momenta is provided by a specified angle of incidence of the optical probing beam on a plate, so that the azimuth of polarization of this beam coincides with the main optical axis of the birefringent plate. Taking into account all the mentioned factors has convincingly visualized the unconventional motions of a microplate in the field of an evanescent wave.

Optics EXPRESS

2. Determination of optimal experimental conditions

To demonstrate the mechanical action of transversal spin currents [16] inherent in the evanescent wave, we use a plane incident wave (at the interface birefringent plate–air) with the azimuth of polarization $\pm 45°$ with respect to the z-direction, as it is shown in Fig. 2. With the mentioned azimuthal polarization, one achieves the highest magnitude of ellipticity, while the magnitudes of the polarization components of the beam parallel and perpendicular to the plane of incidence are equal. As mentioned above, the test-object is a birefringent microplate, and the total internal reflection (TIR) is realized at the outer surface of a plate, at the plate-air interface. An evanescent wave is excited just above the plate. A transverse diagonal polarization-dependent force of an evanescent wave can be transferred to the plate inducing its motion.

One can specify the following influencing factors:

i) Torque arising as a result of phase difference between ordinary and extraordinary components of the probing wave that leads to changing the AM and consequently a rotation of the plate;

ii) Torque inherent in a circularly polarized wave or circular component of an elliptically polarized wave (internal spin angular momentum);

iii) Extraordinary spin AM of an evanescent wave [11] arising above the plate surface, being included in the complex hierarchy of the local momentum and spin distributions, here transferred to the plate with gold nanoparticles also causing plate rotation and rectilinear motion.

Let us perform qualitative (as possible, quantitative) estimation of the mentioned factors step by step.

i) Let us start our consideration from computing the torque moments resulting from birefringence into the plate owing to the phase difference ordinary and extraordinary components of the probing wave.

In general, torque inherent in a plane, elliptically polarized light wave of angular frequency ω [21] can be calculated by integration over the entire space, where $\tau = \int (\vec{r} \times < \vec{\vec{T}} >) \cdot \hat{n}\, d^2 r,$ where

$$< \vec{\vec{T}} > = [\varepsilon_0 \vec{E} \otimes \vec{E}^* + \frac{1}{\mu_0} \vec{B} \otimes \vec{B}^* - \frac{1}{2}(\varepsilon_0 \left|\vec{E}\right|^2 + \frac{1}{\mu_0} \left|\vec{B}\right|^2) I] \qquad (1)$$

is the time-averaged Maxwell stress tensor in SI-units determining the interrelation between the optical forces and the mechanical moment. Here $\otimes$ is the dyadic product, I is the unit matrix, $\hat{n}$ is the surface-normal vector, $B = \sqrt{\varepsilon \varepsilon_0} E$ is the magnetic inductance vector, and ε is the media permittivity.

Optics EXPRESS

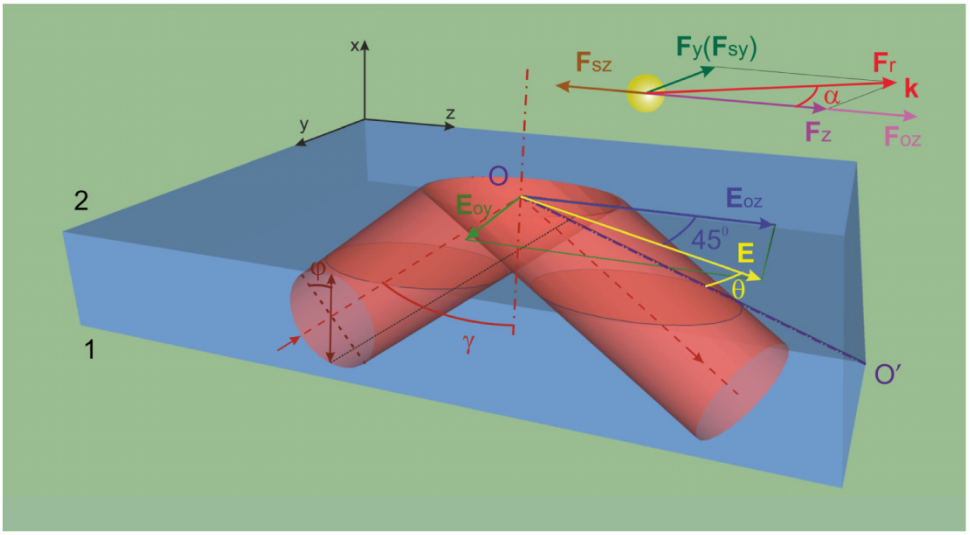

Fig. 2. Notations for the analysis of the propagation of a wave in a birefringent plane-parallel microplate with gold nanoparticles at upper surface. Lower part: OO' – optical axis of a plate: γ – angle of incidence at surface 2 (interface plate-air), φ is the azimuth of polarization of the probing beam, θ – is the angle between optical axis of a plate and the azimuth of polarization of the wave 45° impinging on a surface 2. Upper part represents distribution of forces in the evanescent wave acting on gold particles deposited at the surface of birefringent plate: F_{oz} – force caused by the canonical orbital momentum, F_{sz} – longitudinal component of a force caused by the vertical spin momentum, F_z – longitudinal resulting optical force, $F_y\,(F_{sy})$ – transversal component of a force caused by the vertical spin momentum, F_r – resulting optical force in $\vec{k}$ -direction causing rectilinear motion of the plate. The angle α between directions z and $\vec{k}$, in our case is about 15°.

Let the plane YOZ coincide with the plane of the plate, cf. Figure 2. The linearly polarized plane probing wave is of the azimuth of polarization φ with respect to the plane of incidence. The probing beam forms a spot of area S at the plate. The electrical strength of the probing beam, E_0, is determined by its power P, as $\frac{P}{S}=\frac{\varepsilon_0 c}{2}E_0^2$ or $\frac{P}{S}=\frac{c}{8\pi}E_0^2$, within the Gaussian system.

Beam propagation through the birefringent plate is accompanied with a phase shift between the orthogonally polarized components depending on plate thickness d and refraction coefficient $m=n+i\kappa$ (for birefringence n (n_o, n_e)), where κ – extinction coefficient. Rotation of a plate an angle θ with respect to the optical axis of the crystal causes a change of orientation of the polarization ellipse with associated change of the refraction index, $n_e'=\left(\frac{\sin^2\theta}{n_e^2}+\frac{\cos^2\theta}{n_o^2}\right)^{-1/2}$, causing an induced path difference between the orthogonal components. Therefore, the optical path difference in the plate is likewise changed being determined by the direction of propagation of the beam in the plate, γ, so that, generally, an elliptically polarized wave with the electrical vector

$$\vec{E}_{\text{inc12}}=\left(\vec{y}E_y(\cos\Theta\cos\Phi+i\sin\Phi\cos\Theta)\exp(ikn_o d/\cos\gamma)\exp(-k\kappa d/\cos\gamma)+\right.$$
$$\left.\vec{z}E_z(\sin\Theta\cos\Phi-i\cos\Theta\sin\Phi)\exp(ikn_e' d/\cos\gamma)\exp(-k\kappa d/\cos\gamma)\right)\exp(-i\omega t) \quad (2)$$

Optics EXPRESS

impinges on the second surface of the plate (surface 2 in Fig. 2). Here Φ is the degree of ellipticity of the polarization [22] defined as the tangent of the ratio of the minor to major axes of an ellipse, Θ is the angle between the optical axis and the major axis of the ellipse of polarization, and k is the free-space wavenumber.

Here $E_y = E_0 \sin\varphi(\cos\theta\cos\varphi + \sin\varphi\sin\theta)$, $E_z = E_0 \cos\varphi\cos\psi(\sin\theta\cos\varphi - \cos\theta\sin\varphi)$, where ψ is the angle of incidence to the initial surface (surface 1) of the plate.

Precise qualitative measurements of the action of optical forces within the framework of this model are difficult due to the influence of many factors of the plate motion (optical forces, surface tension of a water etc.). Due to this, we estimate the relative contributions of the longitudinal and transversal components of the optical forces, where their absolute magnitudes are irrelevant.

For computation of the torque induced in the birefringent plate we assume a beam aperture 6°, determining the area of the focused beam at the plate and, correspondingly, the area of integration. A plate is divided into nanometer layers for which one computes a torque τ_{12i}. This approach facilitates taking into account the changing ellipticity for each layer. The resulting torque is found by the summation $\tau_{12} = \sum_i \tau_{12i}$, where i is the number of the layer.

After reflection from surface 2 at the boundary plate-air, cf. Figure 2, the beam propagates in reverse direction, to surface 1 governed by the condition of TIR, with phase shift $\delta = \delta_p - \delta_s$ between the orthogonal components determined by the angle of incidence at the boundary plate-air γ. As a result, a wave with the electrical vector

$$\vec{E}_{\text{inc}21} = \left(\vec{y}E_y(\cos\Theta\cos\Phi + i\sin\Phi\sin\Theta)\exp(i2kn_o d/\cos\gamma)\exp(i\delta)\exp(-k\kappa d/\cos\gamma) + \vec{z}E_z(\sin\Theta\cos\Phi - i\cos\Theta\sin\Phi)\exp(i2kn_e' d/\cos\gamma)\exp(-k\kappa d/\cos\gamma)\right)\exp(-i\omega t) \quad (3)$$

propagates in the reverse direction. By analogy with the torque τ_{12}, one computes the resulting torque, $\tau_{21} = \sum_i \tau_{21i}$. Changing the incidence angle leads to a change of the resulting torque, $\tau = \tau_{12} + \tau_{21}$.

Thus, these changes depend extensively on the rotation angle of a plate with respect to its initial orientation. For visualization of the action of the vertical spin, we intentionally look for the condition, i.e. the combination of magnitude of the two parameters, viz. the incidence angle and the angle of plate rotation, for which the optical force is largest. Thus the action of the vertical spin becomes evident if the plate rotation stops. This occurs when

(i) under the plate rotation the azimuth of linear polarization (45°) of the incidence beam coincides with the plate axes;

(ii) the compensation of the resulting torque τ caused by the birefringence of a plate is achieved. Figure 3 illustrates the results of simulation of torque for the beams propagating to the boundary plate-air (curve 1) and from this boundary (curve 2). Curve 3 in Fig. 3 corresponds to changing of torque $\tau = \tau_{12} + \tau_{21}$.

It has been found that compensation of torque is provided for incidence angles 51.5° and 58.5° when averaging over a beam aperture 6°. We here choose an incidence angle of 58.5°.

Subsequently, any movement of the plate can be explained by the direct action of an evanescent wave, solely by the mechanical action of the vertical spin arising for the azimuth of polarization ± 45° of the incidence beam on the surface 2.

Optics EXPRESS

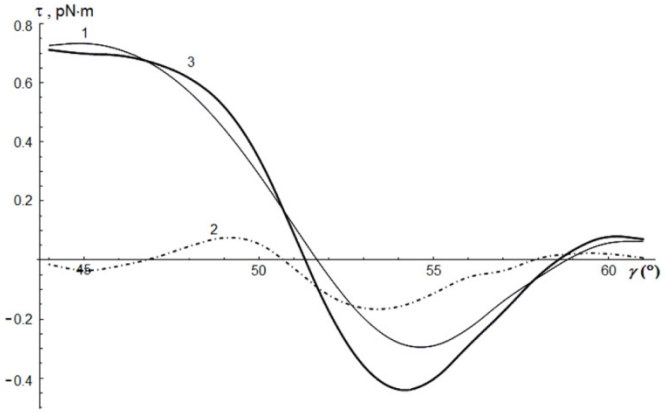

Fig. 3. Dependence of the torque on the angle of incidence γ of the beam impinging on the second surface of a plate, for which one of the plate axes coincides with the azimuth of polarization of the incident beam 45°: Curves 1 and 2 correspond to the torque of the beam propagating to the boundary plate-air and from this boundary, respectively; curve 3 represents the resulting torque.

ii) The next step of simulation consists in estimation of the optical force resulting from the spin moment density inherent in circularly polarized wave and the optical force resulting from birefringence into the plate.

Therefore we have computed the spin momentum inherent in circularly polarized wave arising in a birefringent plate for a beam propagating to the surface 2 (Fig. 2) and from this surface as a result of TIR. Accordingly [2], the density of the spin and orbital momentum are defined as $\vec{p}_s = \frac{1}{16\pi\omega}\mathrm{Im}\left[\nabla\times(\vec{E}^*\times\vec{E})\right]$ and $\vec{p}_o = \frac{1}{8\pi\omega}\mathrm{Im}[\vec{E}^*\cdot\nabla\vec{E}]$. Here, $\vec{E}$ is the electrical strength of the circularly polarized wave represented by $\vec{E}_{inc12}$ and $\vec{E}_{inc21}$. This facilitates deriving the orbital and spin momentum for beams propagating to the outer surface of a plate and from this surface. Transfer of the orbital and spin momentum density to the plate [23] causes the optical force leading to a plate motion $\vec{F} = \int \vec{p}\, dS$. The results of simulation show that the magnitude of an optical force associated with a transfer of the classical spin momentum, F_s, inherent in circularly polarized wave and arising in the plate due to birefringence, is considerably less than the force induced by birefringence, F_{br}, so that $F_s / F_{br} \approx 10^{-10}$. Thus, the force caused by the spin momentum density does not affect the moving plate.

iii) At last, under the above determined conditions, we compute the magnitude of the optical force arising from the evanescent wave above the surface of a birefringent plate. Formation of elliptically polarized wave at the super surface layer enables us to estimate the longitudinal and transversal components of the force. Therefore, the vertical spin of an evanescent wave is the source of the last of them.

Thus we simulate the spin and orbital momenta inherent in an evanescent wave when a linearly polarized incidence wave (at surface 2) with the azimuth of polarization 45° reaches the interface plate–air here undergoing TIR. In this case, an evanescent wave that propagates in the z-direction, being damped in the x-direction, can be represented by [16, 24]

$$\vec{E}_{\mathrm{ev}} = E\exp(-i\omega t)\left(\vec{x}\frac{1}{\sqrt{1+|m|^2}} + \vec{y}\frac{m}{\sqrt{1+|m|^2}}\cdot\frac{k}{k_z} + \vec{z}(-i)\frac{1}{\sqrt{1+|m|^2}}\frac{\kappa}{k_z}\right)\cdot\exp(ik_z z - \kappa x), \quad (4)$$

Optics EXPRESS

where $k_z = k\frac{n_o}{n}\sin\gamma$, $\kappa = k\sqrt{\left(\frac{n_o}{n}\right)^2 \sin^2(\gamma) - 1}$ is the exponential decay rate.

The state of polarization of an evanescent wave [16] is $m = \frac{T_\perp}{T_{//}} m_1$, where m_1 is the state of polarization of the probing beam impinging at the interface plate–air being equal to unity for linear polarization with the azimuth of polarization 45°. γ is the angle of incidence at the surface, where TIR takes place.

The electrical strength of the field of an evanescent wave is $E = \frac{k_z}{k}\sqrt{\frac{\mu_1}{\mu}} T E_0$, where $T = \frac{\sqrt{|T_{//}|^2 + |m_1|^2 |T_\perp|^2}}{\sqrt{1+|m_1|^2}} \exp[i \arg T_{//}]$ is the transmission coefficient [16], and $T_{//}$, $T_\perp$ are the Fresnel transmission coefficients.

The orbital momentum is expressed as $p_o = \frac{1}{8\pi\omega} \mathrm{Im}[\vec{E}^*_{ev} \cdot (\nabla) \vec{E}_{ev}]$. The orbital (canonical) momentum caused by light pressure determines a force transferred to the plate in the direction of propagation of an evanescent wave, here in the z-direction.

An evanescent wave excited at the boundary plate-air induces the spin angular momentum that is transferred to the plate causing rotation. This torque is characterized by the z- and y-directions.

The spin momentum density in this case is expressed as [11,16] $p_s = \frac{1}{16\pi\omega} \nabla \times \mathrm{Im}[\vec{E}^*_{ev} \times \vec{E}_{ev}]$, having both longitudinal and transversal components [11]. Thus, the resulting momentum density in the z-direction is given by

$$p_z = p_{oz} + p_{sz} = \frac{A^2}{8\pi\omega}\left[\left(k_z + \frac{m^2 k^2}{k_z} + \frac{\kappa^2}{k_z}\right) - 2\frac{\kappa^2}{k_z}\right]\exp(-2\kappa x) \qquad (5)$$

and the transversal momentum caused by the vertical spin is represented as $p_y = p_{sy} = \frac{A^2}{4\pi\omega}\frac{k\kappa}{k_z}\mathrm{Im}\, m \exp(-2\kappa x)$, where $A = E\frac{1}{\sqrt{1+|m|^2}}$.

Changing the angle of incidence of a beam at the boundary plate-air leads to changing the ellipticity of the evanescent wave excited above the plate surface. That is why one can assume that the magnitude of the transversal spin momentum could be characterized by the different dependence with respect to the resulting momentum in the longitudinal direction, where the main contribution is provided by the canonical momentum. We assume that the momentum is transferred by the spherical surface S of the gold particles localized at the plate surface. Light-scattering by particles is taken into account within the Mie approximation [16], giving $\vec{F} = \int_s \Delta\vec{p} dS$, where $\Delta\vec{p}$ is the change of momentum density. Simulation of the force affecting a plate and causing its motion presumes integration over the illuminated area assuming a beam aperture 6°. The results of simulation of optical forces induced in the y- and z-directions for a linearly polarized incident beam with the azimuth of polarization 45° versus the incidence angle γ are shown in Fig. 4.

Optics EXPRESS

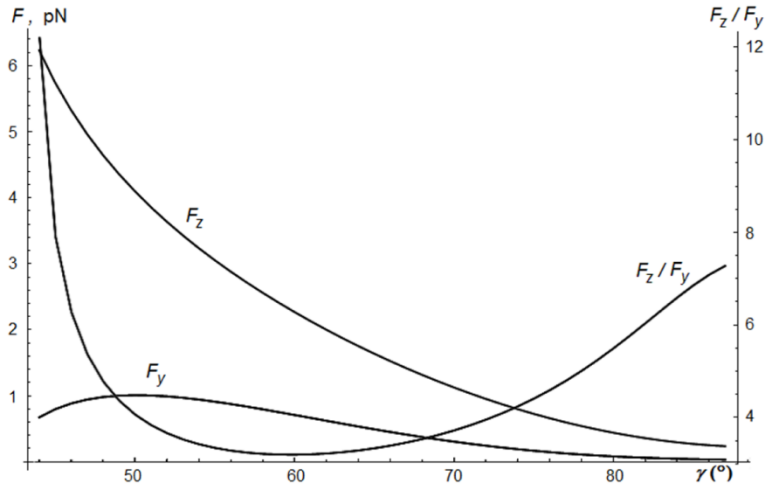

Fig. 4. The resulting force in the z-direction (F_z), the transverse diagonal polarization-dependent force induced by the vertical spin momentum in the y-direction (F_y) and the ratio of optical forces in the longitudinal and transversal directions (F_z / F_y) as a function of the incidence angle γ.

One can see from Fig. 4 that for some incidence angles, the forces in the y- and z-directions are comparable, the angle for which this occurs can be found from this figure. So, as it can be seen from this figure (curve F_z / F_y), for incidence angle about 58° one obtains: $F_z / F_y \approx 3.2$. As we estimate the ratio of the transverse components of a force rather than their absolute magnitudes, this ratio is not influenced by the concentration and size of nanoparticles of the monodisperse system.

This is exactly the angle, for which the momenta caused by birefringence (for the beams propagating to the boundary pate-air and from this boundary) are compensated. That is why one can regard the motion of a plate in a direction different from longitudinal as the result of the action of an optical force, one of the components of which is the force induced by the transversal spin momentum density, see Fig. 2. This statement is experimentally demonstrated.

3. Experiments

The transfer of the momentum from an evanescent wave to the microplate can be realized due to the surface irregularities of the plate. However, in the case of interest here, we use a plate of optical quality (RMS = 2 nm). That is why, for momentum transfer from a laser beam to the plate we use gold 60 nm-diam nanoparticles deposited at the upper surface of the plate facilitating the observation of action of the spin momentum. In absence of gold particles, rectilinear motion is not observed and only rotation of a plate takes place. At one surface of a PETF plate 10x10 mm we deposit a drop (0.1ml) gold hydrosole of 60 nm ± 2 nm diameter. We do not have high-resolution image of the plate surface with nanoparticles, but we are in a position to estimate the particle concentration based on the concentration of gold hydrosole. So, the gold particle concentration at the plate surface is approximately 1 μg/mm^2. To prevent aggregation of gold particles, we apply 30 V electrical potential. As a result of water evaporation from a drop, only uniformly distributed gold particles are kept at the plate surface with concentration 1 μg/mm^2. Subsequently, we cut a plate of size, 200x200 μm, which is used as the test object in our experiment.

Optics EXPRESS

In brief, an evanescent wave is excited at the boundary of a plane-parallel plate, free-standing at a water surface. The significant size of the plate (from 20 to 200 μm) allows for averaging from the Langevin fluctuation of the environment caused by its molecular structure, so that the influence from Brownian movements is negligible. Radiation from a semiconductor laser (980 nm Laser from Wavespectrum, WSLD-980-004-C 980 nm 4 W) is focused at the boundary of the plate and air without spatial-frequency filtering. The rectangular focal spot has a 50 μm cross-section. The cone angle of the beam is 6°. In this case, it is not necessary to take into account the gradient forces, as a plate is statistically homogeneous and a beam is focused within the plate. We are in a position to control the azimuth of linear polarization of the probing beam by turning the illuminator. In such a way, we control the beam polarization at the boundary plate-air.

The use of a high-energy laser beam causes temporally induced flows. However, convection flows are localized within a cuvette, in a water environment. At the same time, a micro particle is kept at the water surface due to surface tension. Clear verification of this statement is provided in Visualization 1 where one can see that a plate of 7 μm-thickness aluminum foil is neither rotated nor moves rectilinear in the same optical arrangement even for doubled beam intensity (2W). For polished surface of an aluminum plate, the action of the optical forces at the plate plane is negligible, so that any motion may be associated with the processes in water, including ones caused by heating of water and plate by laser radiation.

We neglect the influence of the convection flows in water, as for the same optical arrangement but with doubled power of the probing beam a plate from aluminum foil does not rotate and does not move forward, though heating of both water and aluminum plate is larger than in the case of the PETF plate (Visualization 1). For smooth surface of the aluminum plate, optical forces must be negligible, and any of its motion would be associated with the processes in water due to heating of water and plate by laser radiation.

The motion of a plate is considerably moderated by the surface tension of the liquid. The superficial region of the liquid is rather thin. Nevertheless, one can in this region clearly observe the influence of long-range molecular connections. So, the presence of hydrogen connections at the water surface is demonstrated in Fig. 2 in the main text body, Fig. 5 (Visualization 2, 19 to 33 sec), where one can see movement of a plate with laser illumination [Fig. 5(a)] and its returning into the initial position when the laser radiation is blocked [Fig. 5(b)]. The net of hydrogen connections of water surface is strongly coupled with a plate being deformed but not destroyed under plate movement. So that blocking out of laser radiation and annulling optical forces lead to movement of the plate to its initial position. As beam power increases to 2 W, the plate velocity doubles, approximately (Visualization 2).

To increase the sensitivity of the arrangement, one must diminish the influence of the surface tension of water. This can be achieved in two ways: (i) control of the form and steepness of the meniscus at the upper region of a cuvette; (ii) heating of the liquid. It is known that convex meniscus decreases surface tension of water. Thus, we aspire to this case when a particle does not return to its initial position and is left immovable when the laser radiation is blocked. It has been found that an optimal meniscus has a curvature radius of 57 mm. For larger meniscus curvatures, a plate moves from the center of the cuvette to its boundary, while for smaller curvature a plate tends to return to its initial position due to surface tension forces.

We also carried out experiments with liquids with considerably less surface tension, such as alcohol, acetone, and water solutions of these. Unfortunately, in these cases the results are strongly inflicted by noise from light-scattering. This effect can be observed in Visualization 3 for a cuvette with 100% ethyl alcohol showing intense dynamical light-scattering. At room temperature alcohol cannot be of 96% purity, and as seen steam is evaporating from alcohol.

In the second case, laser radiation is absorbed by water and subsequently heated resulting in diminishing surface tension and manifestation of optical forces caused by the evanescent

Optics EXPRESS

wave. Note, water strongly absorbs at wavelength 980 nm where the extinction coefficient equals 0.43 cm-1.

We use a 1.3-megapixel CCD-camera without cover glass for IR region, and are thus in a position to observe both the plate illuminated within the visible range as well as position of IR beam at the plate. The power of the laser radiation is changed from 0.1 W to 3 W. Note, for high power of the probing beam, one observes strong scattering at TIR by gold particles at the boundary plate-air.

We use as a test-object plates of 9 μm-thickness polyethylenetereftalat (PETF), $n_o = 1.54$, $n_e = 1.62$, with a birefringence of 0.085. The PETF plate is a two-axis crystal. Bisectrix between its crystalline axes are orthogonal to the plate surfaces. A plate can be considered as a birefringent phase plate, two orthogonal axes of which lie at the plate plane. Choice of PETF plates ensures investigation of a large suite of including the forces caused by birefringence, the mechanical action of light pressure and transversal spin of an evanescent wave. We use non-reflecting, non-absorbing anisotropic dielectric plate. An absorbing plate would diminish the action of the optical forces due to diminishing portion of the incident radiation passing a plate.

Following from the mentioned conditions for realization of the experimental observation of the plate motion, one can conclude that rectilinear motion of a PETF plate can be explained by action of the optical force caused by longitudinal and transversal components of the spin momentum density of an evanescent wave excited by the linearly polarized beam with the azimuth of polarization of ± 45° [13,15].

The illuminated plate rotates and moves rectilinearly (Fig. 5, Visualization 2). Note the direction of rotation depends on the azimuth of polarization of the linearly polarized probing beam as well as on the orientation of the optical axis of the plate. PETF plate can rotate due to circularly component of elliptically polarized beam (birefringence of a plate), and rectilinear movement is caused by an evanescent wave, i.e. the optical forces induced by light pressure and transversal component of the vertical spin momentum.

Experimental study has shown that the motion of the PETF plate depends significantly on the angle of incidence of the beam generating the evanescent wave. The incidence angle affects both velocity and direction of rotation of the plate, as well as the angle of deviation of the forward movement from the z-axis.

The motion of a PETF plate with size 200 μm is demonstrated in Fig. 6 (Visualization 4). Adjusting the incident beam to the centre of the PETF plate is performed at low beam power (about 20 mW), which is observed at the beginning of the video. Such power level does not result in a movement of the plate. Increasing the power of the beam up to 1 W leads to movement of the plate. One observes simultaneous plate rotation and forward movement. The rotation of the plate stops, cf. Figure 6, when the main optical axis of the plate coincides with the azimuth of polarization of the incident beam, continuing the rectilinear motion until the beam leaves the plate. Rotation vanishes precisely for linearly polarized wave impinging onto the surface 2 of a plate at an angle ± 45°, due to birefringence torques being compensated. This is achieved for an angle of incidence of the probing beam about 58° which gives the azimuth of polarization of this beam at interface 1 in Fig. 2 equal 62°. Therefore, rectilinear motion of a plate without rotation has the transversal component due to the transversal component of the vertical spin i.e. a plate slightly shifts in transversal direction due to the transversal component of the vertical spin momentum. The angle between the motion direction and z-axis is 15°, approximately, which correlates with the ratio of forces acting on the plate F_z / F_y shown in Fig. 2. It is reasonably to compare Fig. 4 and Fig. 6, as well as Visualization 4 and Visualization 2.

Optics EXPRESS

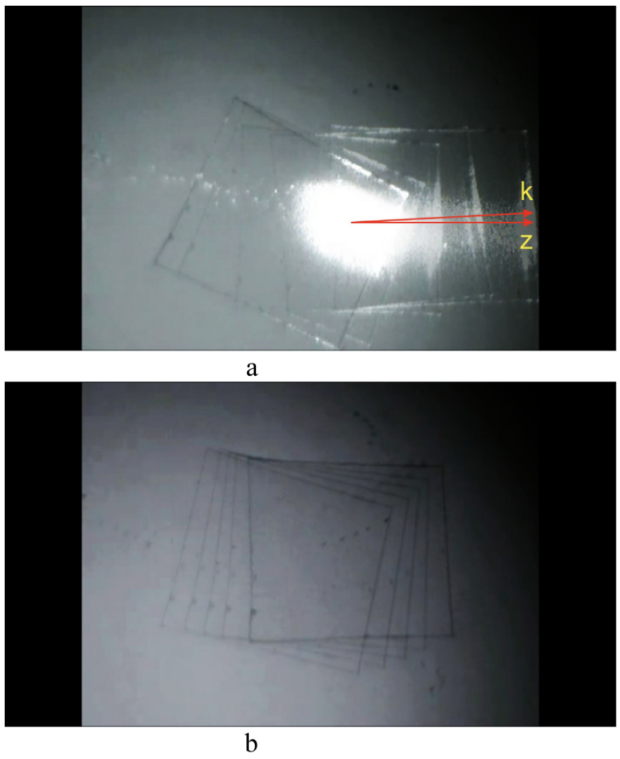

Fig. 5. Motion of a plate illuminated by laser radiation: rotation and rectilinear motion of a plate with 1W-power laser radiation (a); returning the plate into initial position when the laser is turned off (b) (see Visualization 2).

In the second case, the angle of incidence of the beam equals 45°, causing a larger magnitude of the longitudinal component of the optical force caused by the orbital momentum density and, as a consequence, less contribution of the transversal component of the force caused by the spin momentum as shown by their ratio in Fig. 3 ($F_z / F_y > 10$). That is why a plate moves practically along the z-axis with higher velocity, despite the presence of the surface tension of water.

Let us emphasize that the direction of motion of a microplate does not depend on the position of the laser spot. The main condition is that the spot must be focused within the plate to avoid edge effects. This is clearly seen in Visualization 2 and Visualization 4. When a microplate moves rectilinearly, the spot position is changed from the center of a plate to its edge, which does not affect the rectilinear motion. At the final stage of rectilinear motion of a microplate, the spot partially exits the plate. But even this effect does not affect rectilinear motion of a particle. This supports the assumption of the relatively weak influence of the edge effects on the plate motion.

Note, one can observe in Figs. 5 and 6 illuminations of the microplate's edges resulting from illumination of edges by light scattered by gold nanoparticles. As the size of gold particles is much less than a wavelength of laser radiation (by 8 times, approximately), the scattering indicatrix is spherical, so that only a small portion of the total intensity is scattered within any direction (within a small solid angle). That is why the main contribution to the plate motion is caused by the light momentum transferred to gold particles. Waveguide effect in a microplate is negligible, as the interface 'plate-water' is characterized by small relative refraction index and reflects less than 10% of the intensity of radiation.

Optics EXPRESS

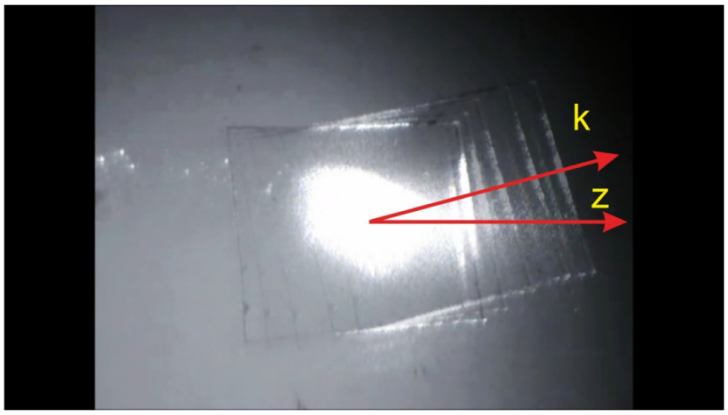

Fig. 6. Rotation and rectilinear motion of a plate at an angle of 15°, approximately, to the z-direction induced by 1W-power laser beam impinging on a plate at an angle of 58° (see Visualization 4).

Thus, the use of a PETF plate for demonstration of the action of optical forces, including various components of the spin and orbital momentum density, is successfully realized, as one can see from the results of both computer simulation and the physical experiments.

Conclusion

In this paper we have for the first time demonstrated the action of ordinary and extraordinary spin on birefringent microplates, providing one more obvious proof of the existence of the extraordinary (transversal) spin. We have demonstrated the motion of a birefringent plate in a direction controlled by simultaneous action of the canonical momentum (directed along the wavevector) and the transversal spin momentum under exceptionally delicately determined experimental conditions, when the contribution of the canonical and spin momenta in determination of the trajectory of the resulting motion occur commensurable, and the chaotic influence of motion of molecules is diminished due to averaging over the plate area. At the same time, the influence of surface tension of water has been minimized by using a convex meniscus. Commensurability of the contributions of the optical force caused by the simultaneous action of the canonical and the transversal spin momenta have been achieved by proper choice of the angle of incidence of the optical beam at the interface birefringent plate–air in the case when the azimuth of polarization of the beam (45°) coincides with the main optical axis of the birefringent plate material.

Acknowledgments

The authors are grateful to Prof. A.Ya. Bekshaev and Prof. K.Ya. Bliokh for useful discussion of the topic of this work.